International Journal of Concrete Structures and Materials

RESEARCH Open Access

Evaluation on Properties of Cement Mortar and Brick Using Magnetically Separated Coal Power Plant Bottom Ash

Ji-Hyun Kim[1], Hoon Moon[2] and Chul-Woo Chung[3*]

Abstract

Recycling of abandoned waste bottom ash has been a key issue in Republic of Korea in terms of environmental protection as well as economic concern. In this work, a method for recycling of abandoned bottom ash has been discussed based on the results from laboratory and industrial-scale experiments. Abandoned bottom ash was magnetically separated and properties of magnetically separated bottom ash samples as well as properties of mortar and masonry cement brick made of bottom ash were investigated. According to the experimental results, bulk and skeletal densities were ranked in the order of strongly magnetic > weakly magnetic > as-received > non-magnetic (from heavier to lighter) bottom ash. From laboratory-scale experiments, compressive strengths of mortars made of bottom ash samples (measured by ASTM C 109) were lower than that of mortar made of standard sand. Among bottom ash samples, mortar made of non-magnetic bottom ash (after removal of unburnt carbon) showed higher compressive strength with lower thermal conductivity (measured by ASTM C 1113) and weight than others. Masonry cement brick made of magnetic bottom ash showed lower weight and thermal conductivity than those made of standard sand, while meeting the KS strength guideline as a masonry cement brick. The results suggest the applicability of bottom ash as lightweight aggregate for production of masonry cement brick. However, considering the lower strength obtained from masonry cement brick made of as-received bottom ash (without removal of unburnt carbon), unburnt carbon content should be removed prior to its utilization as lightweight aggregate.

Keywords Bottom ash, Recycle, Magnetic separation, Lightweight aggregate, Masonry cement brick

1 Introduction

Consumption of fossil fuels for operation of coal fired power plant has been consistently increasing all over the world (International Energy Agency, 2009; Korre et al., 2010; Leblond, 2006; Shafiee & Topal, 2008). Although reduction in CO_2 emission is very critical issue in this industry (Hussain et al., 2022), recycling of waste by-products is as important issue as the reduction of CO_2 emission in terms of environmental protection (Abbas et al., 2020; Bui et al., 2019; Lee et al., 2020; Meek et al., 2021; Oakes et al., 2019) considering the amount of waste that has been generated so far. Approximately 730 million tons of bottom ash (Abbas et al., 2020) and 600 million tons of fly ash (Çiçek & Çinçin, 2015; Nyale et al., 2013) are annually produced in the world. Although fly ash has

Journal information: ISSN 1976-0485 / eISSN 2234-1315.

*Correspondence:
Chul-Woo Chung
cwchung@pknu.ac.kr
[1] Multidisciplinary Infra-Technology Research Laboratory, Pukyong National University, Yongso-ro 45, Nam-gu, Busan 48513, Republic of Korea
[2] Korea Institute of Civil Engineering and Building Technology, Goyang-daero 283, Ilsanseo-gu, Goyang-si, Gyeonggi-do 10223, Republic of Korea
[3] Division of Architectural and Fire Protection Engineering, Pukyong National University, Yongso-ro 45, Nam-gu, Busan 48513, Republic of Korea

been successfully utilized as a supplementary cementitious material due to its beneficial properties such as reduction in the heat of hydration (Atiş, 2002a, 2002b; Langan et al., 2002; Matos et al., 2020; Nocuń-Wczelik, 2001; Schindler & Folliard, 2005), improvement in workability (Atiş, 2002b; Leung et al., 2016; Nocuń-Wczelik, 2001; Uysal et al., 2012; Yao et al., 2015), and long-term strength and durability (Pala et al., 2007; Siddique, 2003; Tikalsky et al., 1988), most of the bottom ash has not been recycled and abandoned in the waste storage site.

The utilization of bottom ash as a supplementary cementitious material has been limited. The chemical compositions of bottom ash are similar to that of fly ash. However, the particle size is larger and the structure is more crystalline than fly ash. For this reason, the pozzolanic activity of bottom ash is very weak. The work of (Cheriaf et al., 1999) showed that bottom ash did not react with calcium hydroxide at early ages. The pozzolanic activity was very slow until 28 days, and became accelerated after 90 days. Jurič et al. (Jurič et al., 2006) recommended to replace up to 15 wt% of cement by bottom ash to use it as a supplementary cementitious material. Kula et al. (Kula et al., 2002) showed that bottom ash can be used as a supplementary cementitious material depending on its particle size distribution. Jaturapitakkul et al. (Jaturapitakkul & Cheerarot, 2003) observed a glassy aluminosilicate phase (diffused halo maxima) at 20–27° 2θ (Cheriaf et al., 1999; Chindaprasirt et al., 2009) that can be a source of pozzolanic reaction, but reported that the pozzolanic activity of bottom ash can be increased by grinding the particle size lower than 45 μm. According to the literature, pozzolanic activity of bottom ash was so slow or weak that it cannot be effectively utilized as a supplementary cementitious material without additional mechanical or chemical treatment (Filipponi et al., 2003; Liu et al., 2018; Mangi et al., 2018).

For these reasons, the use of bottom ash has been focused on the source of aggregate (Andrade, 2004; Andrade et al., 2007; Ghafoori & Bucholc, 1996; Jurič et al., 2006; Wongkeo & Chaipanich, 2010; Yang, 2021). Andrade et al. (Andrade, 2004; Andrade et al., 2007) investigated on evaluation of concrete incorporating bottom ash, as a replacement material for a natural fine aggregate. Ghafoori & Bucholc (1996) also used bottom ash as fine aggregate for structural grade concrete. Results from both works showed that the use of bottom ash required higher water demands and decreased 28 day compressive strength in general. The reason was mainly associated with higher porosity in bottom ash. As a result, many researchers have used bottom ash as a source of lightweight aggregate (Han et al., 2015; Rafieizonooz et al., 2016; Wongkeo & Chaipanich, 2010; Yang, 2021; Zhang & Poon, 2015). Some researchers also studied shrinkage characteristics of cement-based materials using presoaked bottom ash expecting that the water inside the bottom ash can play a role as a water reservoir to prevent drying and autogenous shrinkage (Caprai et al., 2020; Tran et al., 2021).

It was reported that bottom ash contains some amount of hematite and magnetite (Sathonsaowaphak et al., 2009; Šulc et al., 2022; Um et al., 2009; Wei et al., 2017) whose densities were around 5.24 and 5.15 g/cm^3, respectively. If hematite and magnetite phases in bottom ash can be removed effectively, the efficiency of bottom ash as a lightweight aggregate will be increased. It is also important to notice that thermal conductivities of hematite and magnetite are higher than other minerals in bottom ash. According to Mølgaard and Smeltzer (J. MØlgaard & W. W. Smeltzer, 1971), the thermal conductivity of magnetite was in the range of 4.9 ~ 7.0 W/m K while thermal conductivity of hematite was 2 times higher than that of magnetite. Considering the characteristics of ferrous and ferric oxides in bottom ash, the removal of magnetite and hematite will provide the reduction in heat transfer within the skeletal structure of bottom ash, thereby increasing heat insulation capability when used as a lightweight aggregate.

It should be noted that magnetic separation of hematite and magnetite from bottom ash has been attempted by many researchers. However, most of the works were focused at recovery of iron after magnetic separation or related to the investigation on the leachability of heavy metal ions (Boom et al., 2011; Chimenos et al., 1999a; Han et al., 2009; Wei et al., 2017; Yin et al., 2021). Development of a method that can massively utilize magnetically separated bottom ash as a construction material has not been investigated elsewhere. Since most of the hematite can be categorized as weakly magnetic and magnetite can be categorized as strongly magnetic, the sequential application of weak and strong magnets will allow us to separate bottom ash that is (1) strongly magnetic, (2) weakly magnetic, and (3) non-magnetic.

In this research, bottom ash stored in pond site of Hadong coal fired power plant in Republic of Korea has been used. Using magnetically separated bottom ashes, various cement mortar specimens were made to investigate its absorption capacity, compressive strength, and thermal conductivity. Since chemical and mineralogical compositions of bottom ashes can be different depending on the source of coal and its incineration process (Chimenos et al., 1999b), the chemical and mineralogical properties of bottom ash used in this works (before and after magnetic separation) are also investigated. Considering the fact that magnetically separated bottom ash can be used for the production of precast products, lightweight insulation bricks, permeable blocks, and

soundproofing blocks, this work has specific meaning to present a showcase study that can lead to massive consumption of abandoned bottom ashes in the world.

2 Lab-Scale Experimental Procedure

This work consists of two different steps of experimental programs: (1) the experimental investigation conducted in lab-scale and (2) the verification on applicability of magnetically separated bottom ash in industrial-scale. The former contains the investigation on material properties of magnetically separated bottom ash, as well as compressive strength, absorption capacity, and thermal conductivity of mortar made of magnetically separated bottom ash. The latter contains the industrial-scale production of masonry cement brick samples and investigation on the properties of masonry cement brick. Experimental program of this work is summarized in Fig. 1. Based on the experimental results, recommendations for utilization of bottom ash generated from coal fired power plant have been suggested based on the results from lab-scale and industrial-scale experiments.

2.1 Materials

The cement used in this experiment was a commercial ordinary type I portland cement (Ssangyong cement co., Ltd. Republic of Korea) conforming to ASTM C 150 (ASTM C150, 2009). Fine aggregate which was used for comparison with bottom ash was ISO standard sand (CEN EN 196–1 Standard sand) (SNL Co., Ltd. France) that meets the requirements in KS L ISO 679 (KS L, 2006). Bottom ash used in this study was obtained from the coal power plant located at Hadong (pond site) in Republic of Korea. The photographic images of bottom ash used for magnetic separation are presented in Fig. 2. It should be noted that unburnt carbon content of bottom ash in the storage site was found to be 25 wt.%. The chemical compositions of materials used in this work (after removal of unburnt carbon or minor organic constituents) are presented in Table 1.

2.2 Magnetic Separation Process of Bottom Ash

Bottom ash samples that were collected from a pond site were placed at 105 °C oven for 24 h to remove moisture. Oven dried bottom ash samples were sieved using mechanical shaking apparatus consisting of stainless-steel mesh screens with openings of 200 mesh (0.075 mm), 20 mesh (0.85 mm), and 4 mesh (4.75 mm) standard sieves. Bottom ash whose size was larger than 4.75 mm or smaller than 0.075 mm were not used for magnetic separation. The weight proportion of bottom

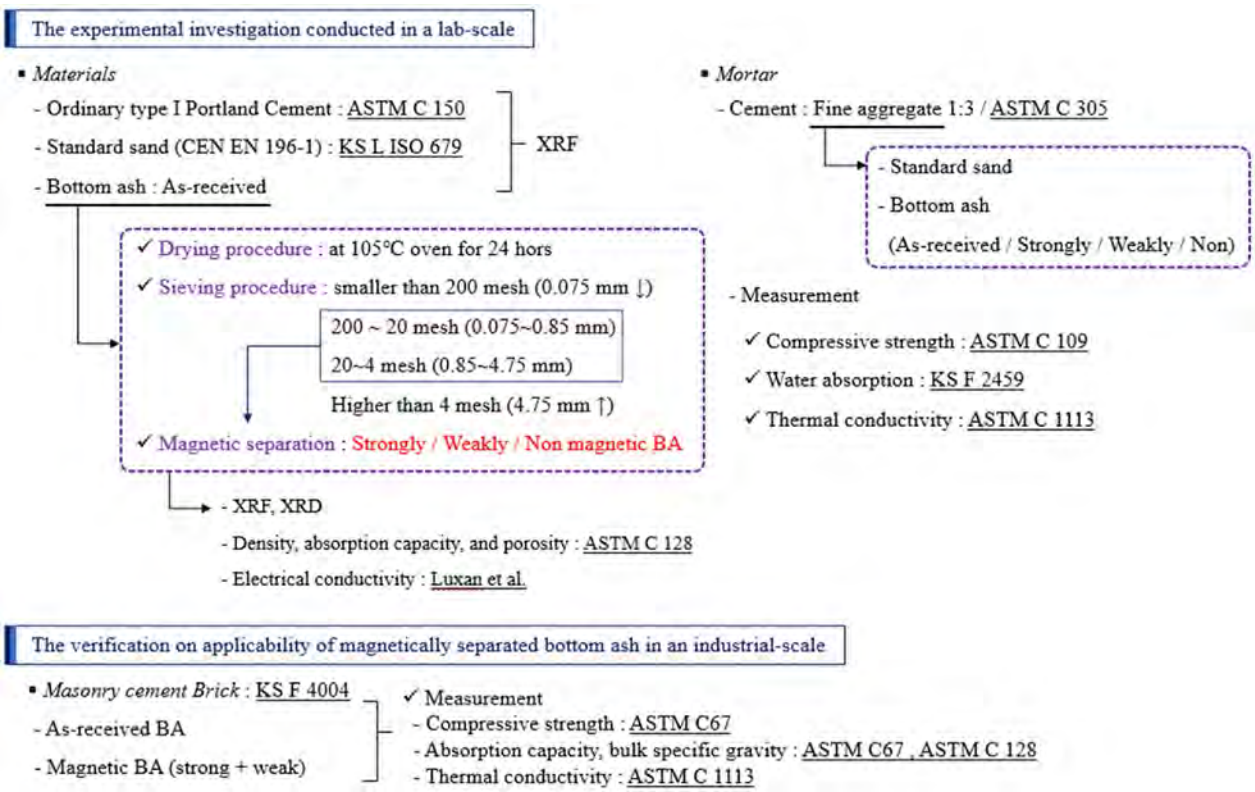

Fig. 1 Summary of experimental program used in this work

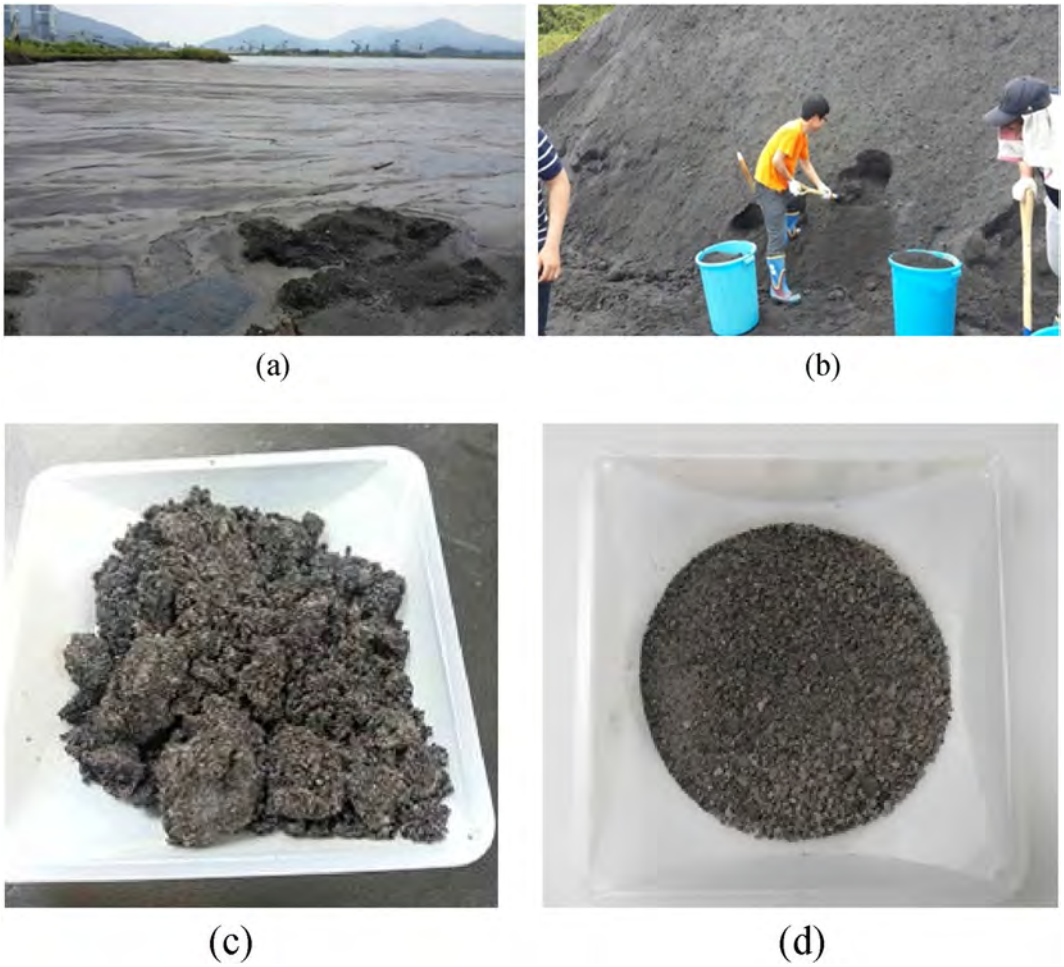

Fig. 2 Photographic images of bottom ash used in this work. Note that (**a**) is an image of pond site, (**b**) is an image during sample collection, (**c**) is an image of as-received bottom ash, and (**d**) is an image of magnetically separated bottom ash after oven drying and sieving

Table 1 Chemical compositions of material used in this work (wt.%)

Material Oxides	Cement	Bottom ash (as-received)	Fine aggregate (standard sand)
SiO_2	17.82	55.09	99.21
Fe_2O_3	2.52	15.91	0.12
Al_2O_3	4.83	13.73	0.09
CaO	66.17	6.11	–
MgO	4.16	2.16	–
SO_3	2.61	2.05	–
Na_2O	–	1.03	–
Cl	–	0.81	–
K_2O	1.13	1.09	–
MnO	0.17	0.23	–
TiO_2	0.31	0.98	–
P_2O_5	0.19	0.70	–
SrO	–	0.10	–
ZrO_2	–	0.02	–

Table 2 Results of sieve analysis of bottom ash used in this work

Particle size	Weight of bottom ash (kg)				wt. (%)
	1st trial	2nd trial	3rd trial	Average	
Higher than 4.75 mm	4.0	4.0	4.0	4.0	10.3
0.85 ~ 4.75 mm	13.0	11.5	11.0	11.83	30.5
0.075 ~ 0.85 mm	21.0	21.5	24.0	22.17	57.1
Smaller than 0.075 mm	0.5	1.0	1.0	0.83	2.1

ash and its unburnt carbon content after sieving are summarized in Table 2.

After sieving, bottom ash samples that were remaining at 4–200 mesh sieves (0.075 ~ 4.75 mm) were magnetically separated. Three types of bottom ashes were separated; (1) strongly magnetic, (2) weakly magnetic, and (3) non-magnetic. For separation of each bottom ashes,

magnetic field of 1000 gauss was first applied to separate strongly magnetic bottom ash samples. In the second stage, stronger magnetic field of 3000 gauss was applied to separate weakly magnetic bottom ash samples. The remaining bottom ash samples were classified as a non-magnetic bottom ash. It should be noted that the unburnt carbon in bottom ash stay together with non-magnetic bottom ash. Therefore, additional sieving procedure was applied to separate unburnt carbon content from non-magnetic bottom ash. Overall magnetic separation process is schematically described as a flowchart in Fig. 3. The weight proportions of bottom ash after magnetic separation are presented in Table 3.

Table 3 The weight proportions of magnetically separated bottom ash

Particle size	Weight proportion of bottom ash (wt.%)		
	Strongly magnetic	Weakly magnetic	Non-magmatic
0.85 ~ 4.75 mm	1.98	1.88	96.14
0.075 ~ 0.85 mm	21.24	3.79	74.96

Considering the data in Tables 2 and 3, the amount of magnetic bottom ash is approximately 15.47% of as-received bottom ash

2.3 Material Characterization After Magnetic Separation

The chemical compositions of bottom ashes before and after magnetic separation (as-received, strongly magnetic, weakly magnetic, and non-magnetic) were analyzed using X-ray fluorescence spectrometer (Simadzu Co., Ltd. Japan, XRF-1700). The mineralogical characteristics of bottom ash samples were analyzed using X-ray diffractometer (Rigaku Co., Ltd. Japan, Ultima IV).

The oven dry (at 105 ± 5 °C) density of bottom ash was measured following ASTM C 128 (ASTM C128, 2015). Skeletal density was measured by placing oven dried (at 105 ± 5 °C) bottom ash in the measuring chamber of helium pycnometer (AccuPyc II 1340, Micromeritics, USA). Since the skeletal density is a density of the specimen without any pores, dividing oven dry bulk density by skeletal density will give total solid volume fraction within bottom ash. Using such correlation, the porosity of bottom ash was calculated by Eq. (1).

$$\left(1-\frac{bulk\ density}{skeletal\ density}\right)\times 100(\%)=porosity(\%) \quad (1)$$

Pozzolanic activity of bottom ash before and after magnetic separation was also evaluated to understand whether there is any difference in pozzolanic activity between magnetically separated bottom ash samples. Electrical conductivity method suggested by Luxan et al. (Luxán et al., 1989) was applied. This method uses 200 ml of 40 ± 1 °C saturated lime solution and 5 g of test

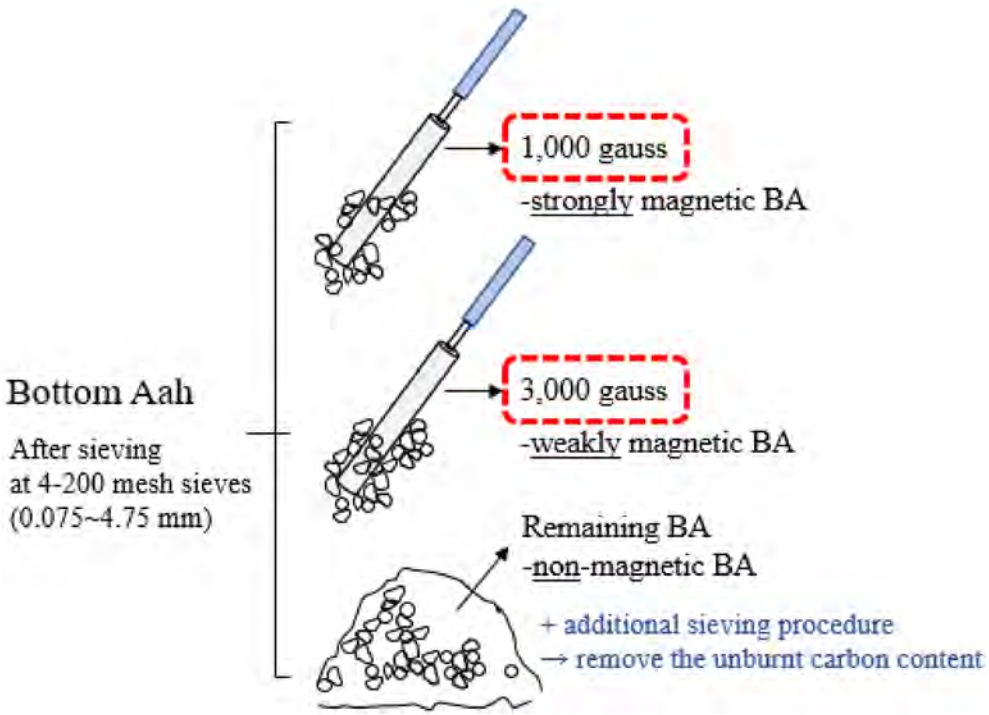

Fig. 3 Schematic illustration of magnetic separation process

material, and drop in electrical conductivity after 2 min was evaluated to characterize pozzolanic activity of test material. In this work, since bottom ash has weaker and slower reactivity, measurement time was extended up to 240 min as reported in our earlier works (Choi et al., 2016; Moon et al., 2017).

As-received and magnetically separated bottom ash samples were finely ground using agate mortar and pestle until particle size became similar to that of cement. Ground bottom ash powder was oven dried at 105 ± 5 °C for 24 h. Saturated lime solution was prepared at 40 ± 1 °C, and initial electrical conductivity was measured. Then, 4 g of powdered bottom ash was immersed and constantly agitated during measurement while maintaining temperature of solution at 40 ± 1 °C. For comparison purpose, fly ash sample that was obtained from the same pond site was also analyzed. The pozzolanic activity can be evaluated as drop in electrical conductivity between initial conductivity and conductivity at 2 min of agitation. Measurement up to 240 min was used for interpretation of long-term reactivity. When the pozzolanic material is immersed in saturated lime solution, a portion of silicate or aluminosilicate reacts with calcium ion to form an insoluble calcium silicate hydrate, thereby reducing electric conductivity (higher drop in electrical conductivity indicates higher pozzolanic activity).

2.4 Preparation of Mortar Specimen

Details of mix proportions of mortar specimens are presented in Table 4. The water to cement ratio (*w*/*c*) was set at 0.4. The volumetric ratio between cement and fine aggregate was 1:3. Mixing of mortar specimens followed the guideline provided by ASTM C 305 (ASTM C305, 2006) using commercial planetary paddle mixer (5KPM50, Kitchen Aid Co. Ltd., U.S.A). Fine aggregate (standard sand or bottom ash) and cement were dry-mixed for 30 s in a mixing bowl. Mixing water and water reducing agent (0.5 wt.% by cement) were added and low speed mix (140 ± 5 r/min) was applied for 30 s. Mixer was stopped for 30 s to scrape down the mortar that was attached to the bottom and side of the mixing bowl. Then, high speed mixing was applied for 60 s at the intermediate speed level (285 ± 10 r/min).

As soon as mixing was finished, fresh mortar was placed in 50 × 50 × 50 mm brass cube molds and 100 × 50 × 20 mm plastic plate mold for measurement of compressive strength and thermal conductivity, respectively. Plastic wrap was placed on top of cast specimens to prevent moisture evaporation, and stored in the ambient laboratory condition (23 ± 2 °C) for 1 day. The molds were removed after 1 day and placed in 23 °C saturated lime solution for 27 days to meet total curing of 28 day.

2.5 Physical Properties of Mortar

The 28 day compressive strength measurements were performed following with ASTM C 109 (ASTM C109, 2008). A universal testing machine (S1 industry Co., Korea, S1-147D) was used for strength measurements. During measurement, the loading rate was maintained at 2 mm/min.

The water absorption of mortar specimen was determined according to the KS F 2459 (2002) (KS F, 2459). The test consists of two major steps: saturating the specimens followed by drying. First, the concrete specimens were immersed in water until the change in mass during 24 h was less than 0.1% (W_{SSD}). Afterwards, the specimens are dried in a ventilated oven at a temperature of 105 ± 5 ℃ until the difference in mass during 24 h is less than 0.1% (W_{OD}). The water absorption can be expressed in Eq. (2) as the amount of water uptake relative to the dry mass:

$$\mathrm{w}(\%) = \frac{W_{SSD} - W_{OD}}{W_{OD}} \times 100 \tag{2}$$

The 28 day thermal conductivity measurements of mortar specimens were performed using a quick thermal conductivity meter (QTM-500, Kyoto Electronics Manufacturing Co. Ltd., Japan) based on ASTM C1113 (ASTM C, 1113–90, 2013). The specimens of 100 × 50 × 20 mm (length × width × depth) were stored in ambient

Table 4 Mix proportions of mortar specimens

No	Sample	*w/c*	Water (*g*)	Cement (*g*)	Fine aggregate (*g*)	
					Sand	Bottom ash[a]
1	Plain	0.4	299.24	748.10	1,959.40	–
2	BA		418.64	748.10	–	1,460.63
3	BA-M		399.64	748.10	–	1,610.25
4	BA-WM		423.54	748.10	–	1,482.00
5	BA-Non		419.44	748.10	–	1,275.40

[a] Refer to the bulk specific ravity of bottom ash presented in Table 6

laboratory condition (23 ± 2 °C) for a day and thermal conductivity of air-dried specimen was measured. Measurement range of the test machine was between 0.020 and 10 W/m K. Measure precision was ± 5% of reading value per reference plate.

3 Results

3.1 Characteristics of Bottom Ash

3.1.1 Chemical Compositions

Table 5 shows chemical compositions of as-received and magnetically separated bottom ash samples. Three major compositions in as-received bottom ash were found to be 55.09% of SiO_2, 15.91% of Fe_2O_3, and 13.73% of Al_2O_3. After magnetic separation, the amount of Al_2O_3 was not affected, but the amount of SiO_2 was reduced. Reduction in SiO_2 content was associated with the increase in Fe_2O_3 content. The amount of Fe_2O_3 in strongly magnetic and weakly magnetic bottom ash was dramatically increased from 15.91% (as-received) to 35.38% (strongly magnetic) and 39.66% (weakly magnetic), respectively. The amount of Fe_2O_3 in non-magnetic bottom ash decreased from 15.91% (as-received) to 9.31%. The results suggest that iron oxides are the main component which allows magnetic separation of bottom ash. The amount of Fe_2O_3 in non-magnetic bottom ash was similar to the amount of Fe_2O_3 in fly ash which was obtained from the same pond site.

3.1.2 Mineralogical Compositions

X-ray diffractometer (XRD) pattern of as-received bottom ash is presented in Fig. 4. It was found that as-received bottom ash contained crystalline phases such as quartz, mullite and cristobalite as well as the presence of an amorphous band at around 17.5 ~ 27.5° 2θ. XRD pattern of fly ash obtained from the same pond site is also presented in Fig. 4. Difference between two materials was the presence of cristobalite and reduction of amorphous band peak intensity, which are indications of crystallization by slower cooling in bottom ash compared to the fly ash. A portion of the amorphous silica was changed to crystalline cristobalite, which can be a cause of weaker pozzolanic activity when used as a supplementary cementitious material. Presence of magnetic phases such as magnetite and hematite were not clearly identified before magnetic separation. This result coincides with the smaller amount of magnetic bottom ash (approximately 15.47% of as-received bottom ash).

X-ray diffractometer (XRD) patterns of magnetically separated bottom ash are presented in Fig. 5. As observed from Figs. 4 and 5, XRD pattern of non-magnetic bottom ash was very similar to that of as-received bottom ash. In general, XRD patterns of strongly magnetic and weakly magnetic bottom ash are almost identical to each other. Non-magnetic bottom ash did not show magnetite. Both magnetic bottom ashes showed strong indications of magnetite, a phase that is responsible for magnetism of bottom ash. More specifically, for bottom ash whose size was 0.85 ~ 4.75 mm (Fig. 5a), magnetite peak intensity of strongly magnetic bottom ash was higher than quartz peak intensity, whereas magnetite peak intensity of weakly magnetic bottom ash was lower than quartz peak intensity. In case of bottom ash whose size was 0.075 ~ 0.85 mm (Fig. 5b), magnetite peak intensities of both strongly magnetic and weakly magnetic bottom ash were almost identical to quartz peak intensity. Hematite and wustite peak intensities from magnetic bottom ash were weak, indicating that these phases were the minor phases in magnetic bottom ash. It is worth noting that the amorphous band around 17.5 ~ 27.5° 2θ in as-received bottom ash was not clearly observed from magnetic bottom ash samples with difference size range.

Table 5 Chemical compositions of magnetic separated bottom ash (wt.%)

Ash Oxides	Fly ash	As-received	Strongly magnetic	Weakly magnetic	Non-magnetic
SiO_2	58.07	55.09	40.35	36.11	63.44
Fe_2O_3	7.02	15.91	35.38	39.66	9.31
Al_2O_3	20.60	13.73	11.88	11.04	13.19
CaO	4.97	6.11	3.49	3.54	4.01
MgO	2.29	2.16	3.31	3.34	2.19
SO_3	0.75	2.05	1.50	1.95	2.05
Na_2O	0.58	1.03	1.16	1.30	1.44
Cl	0.35	0.81	0.83	0.94	1.77
K_2O	1.40	1.09	0.69	0.63	1.21
MnO	0.10	0.23	0.54	0.62	0.16
TiO_2	2.29	0.98	0.49	0.52	0.85
P_2O_5	1.41	0.70	0.34	0.29	0.31
SrO	0.14	0.10	0.05	0.04	0.06
ZrO_2	0.04	0.02	0.00	0.02	0.02

3.1.3 Density, Absorption Capacity, and Porosity

Table 6 summarizes the density, absorption capacity and porosity of the bottom ash after magnetic separation. It should be noted that the skeletal density of as-received bottom ash was 2.71 g/cm^3 and increased to 3.56 and 3.38 g/cm^3 for strongly magnetic and weakly magnetic bottom ashes, respectively. Increase in the skeletal density after magnetic separation was related to the increase in Fe_2O_3 content (Table 5). Therefore, non-magnetic bottom ash which contains the lowest amount of Fe_2O_3, showed the lowest skeletal density of 2.37 g/cm^3.

The oven dry bulk densities and saturated surface dry bulk densities of bottom ash samples followed the same

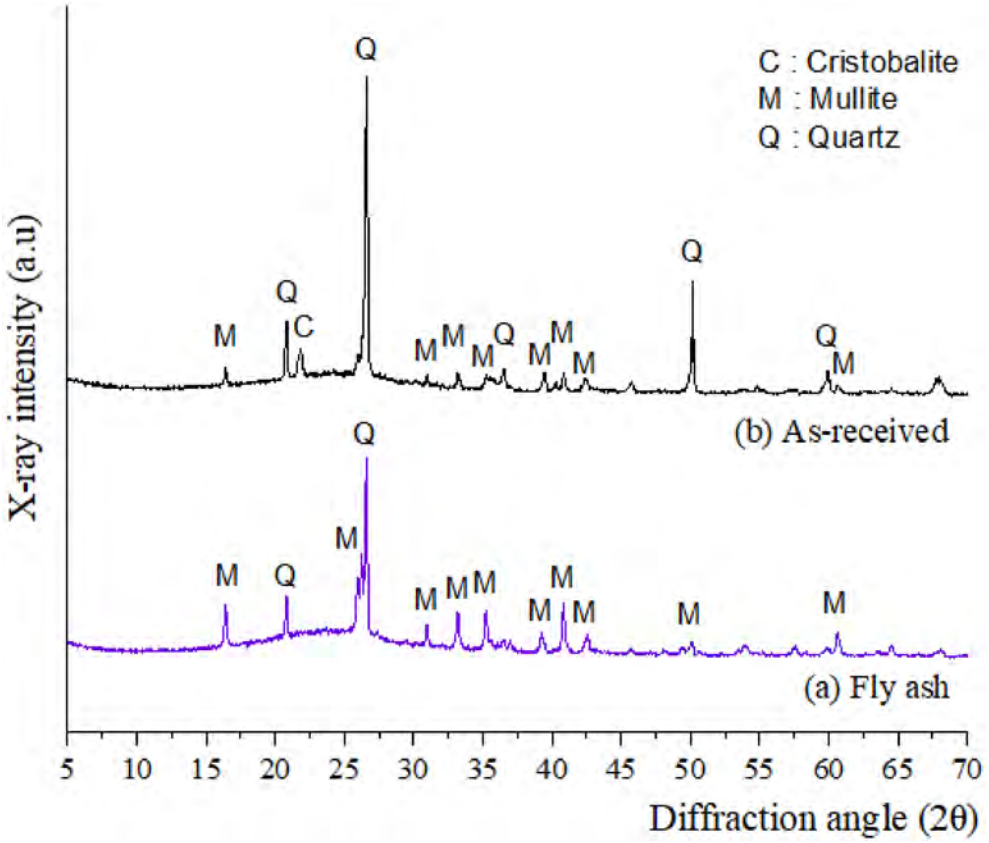

Fig. 4 XRD patterns of bottom ashes: (**a**) fly ash, (**b**) as-received bottom ash. Note that *C* indicates cristobalite, *M* indicates mullite, *Q* indicates quartz, respectively

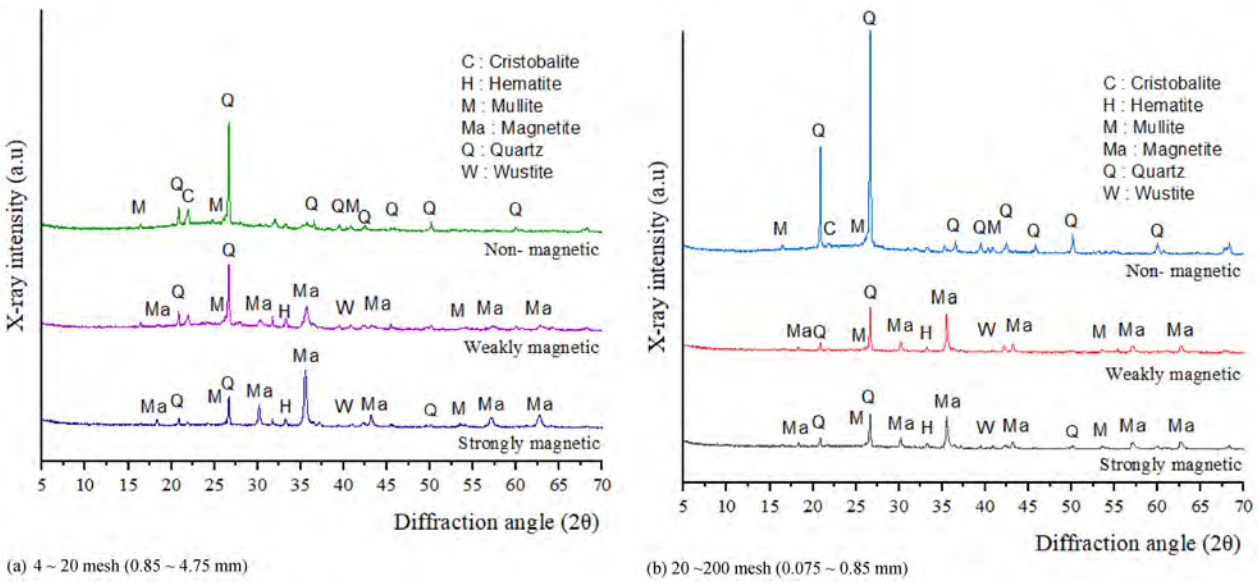

Fig. 5 XRD patterns of magnetically separated bottom ashes: strongly magnetic bottom ash, weakly magnetic bottom ash, and non-magnetic bottom ash. Note that *C* indicates cristobalite, *H* indicates hematite, *M* indicates mullite, *Ma* indicates magnetite, *Q* indicates quartz, and W indicates wustite, respectively

Table 6 Physical properties of bottom ash

Bottom ash Properties	As-received	Strongly magnetic	Weakly magnetic	Non-magnetic
Bulk specific gravity (g/cm^3)—OD	2.05	2.26	2.08	1.79
Bulk specific gravity (g/cm^3)—SSD	2.22	2.40	2.25	1.96
Skeletal density (g/cm^3)	2.71	3.56	3.38	2.37
Absorption capacity (%)	8.20	6.20	8.40	9.40
Porosity (%)	24.35	36.51	38.46	24.47

trend to that of skeletal densities, showing in the order of "strongly magnetic > weakly magnetic > as-received > non-magnetic", from the highest to the lowest. However, absorption capacity and porosity did not follow the same order. The highest absorption capacity was for non-magnetic bottom ash and ranked in the order of non-magnetic (9.40%) > weakly magnetic (8.40%) > as-received (8.20%) > strongly magnetic (6.20%). Porosity was ranked in the order of weakly magnetic (38.46%) > strongly magnetic (36.51%) > as-received (24.35%) ≈ non-magnetic (24.47%). Considering that the difference between porosity and absorption capacity as pores that water cannot be accessed, both strongly magnetic and weakly magnetic bottom ashes contained 30.31% and 30.06% of non-water accessible pores, respectively. It was approximately 2 times as high as that (15.07%) in non-magnetic bottom ash. This could be the reason for smaller differences in bulk densities compared to the skeletal densities.

3.1.4 Pozzolanic Activity

Fig. 6 shows electrical conductivity of bottom ash after magnetic separation. Fly ash samples that were obtained from the same pond site was also analyzed for comparison. It should be noted that the initial electrical conductivity of saturated lime solution without any sample was 7.0 mS/cm. All the samples showed electrical conductivity value higher than 7.0 mS/cm, meaning that some ionic species has been dissolved from bottom ash samples (Paya et al., 2001). This could have been associated with the migration of ionic species from sea water into bottom ash during storage period in the pond site.

In case of fly ash sample, the difference between the initial conductivity and conductivity of saturated lime solution at 2 min after fly ash addition was found to be—0.06. According to the criteria shown in Table 7 suggested by Luxan et al. (Luxán et al., 1989), fly ash stored in the pond site can be evaluated as a non-pozzolanic material. However, it should be noted that fly ash obtained from the pond site showed typical characteristics of low calcium fly ash (mullite, quartz, and amorphous band at around 21 ~ 25°θ without cristobalite). The reason why fly ash did not show pozzolanic activity can be related to the (1) agglomeration of fly ash particles that occurred during storage period in the pond site and (2) dissolution of sea water related ionic species (the same reason as bottom ash) from fly ash that was captured within the structure of agglomerated fly ash particles (Paya et al., 2001). The evidence of particle agglomeration in fly ash is provided in Fig. 7, showing the particle agglomeration in the range of 50 ~ 120 μm, and 330 ~ 700 μm.

Since there was some ionic species that was dissolved from both fly ash and bottom ash samples, the difference between initial electrical conductivity (at 2 min) and final electrical conductivity (at 240 min) was considered as a guideline for evaluation of pozzolanic activity than the guideline (Table 7) suggested by Luxan et al. (Luxán et al., 1989). Fly ash sample from the same pond site showed initial conductivity of 7.06 mS/cm, final conductivity of 4.92 mS/cm, and the difference of 2.14 mS/cm. As-received, strongly magnetic, weakly magnetic and non-magnetic bottom ash samples showed initial conductivities of 7.83, 7.93, 7.92, and 7.78 mS/cm, final conductivities of 6.50, 6.79, 6.69, and 6.64 mS/cm, and the differences of 1.33, 1.14, 1.23, and 1.14 mS/cm, respectively. There was no clear difference in pozzolanic activities among as-received, strongly magnetic, weakly magnetic, and non-magnetic bottom ash samples. Differences between initial and final electrical conductivities (an indication of pozzolanic activity) ranged around 53 ~ 62% of that of fly ash stored at the same pond site. Since pozzolanic activity of fly ash was found to be relatively weaker compared with other reactive pozzolans such as metakaolin and silica fume (Moradllo et al., 2020; Suraneni & Weiss, 2017), also considering that part of fly ash particles was agglomerated so that the pozzolanic activity was evaluated weaker than its full potential, the pozzolanic activity of bottom ash powder can be evaluated either as non-pozzolanic or very weakly pozzolanic. The results indicate that the utilization of bottom ash as a supplementary cementitious material may not be an appropriate direction. The utilization of bottom ash as a lightweight aggregate might be a better alternative.

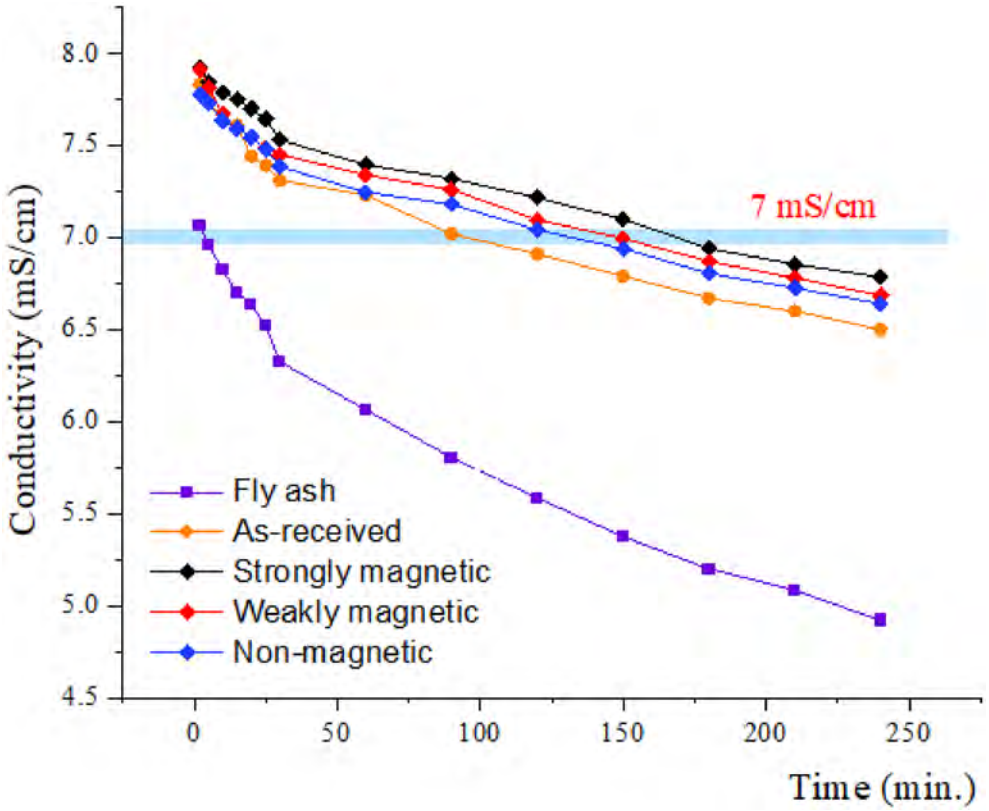

Fig. 6 Electrical conductivities of bottom ash samples after magnetic separation. Note that initial electrical conductivity of saturated lime solution at 40 °C was 7.0 mS/cm

3.2 Characteristics of Mortar with Bottom Ash

3.2.1 Compressive Strength

The 28 day compressive strength of mortar (50 × 50 × 50 mm cube) made of magnetically separated bottom ash are presented in Fig. 8. Due to the higher porosity of bottom ash samples, compressive strengths of mortar made of various bottom ash samples were lower than the strength of mortar made of standard sand. Compressive strength of plain mortar (Plain) was found to be 46.83 MPa whereas compressive strengths of mortar made of as-received (BA), strongly magnetic (BA-SM), weakly magnetic (BA-WM), and non-magnetic (BA-Non) bottom ash were 31.20, 30.02, 36.32, and 36.43 MPa, respectively. Among mortars made of bottom ash, non-magnetic bottom ash showed the highest strength. However, it was only 0.11 MPa higher than that of mortar made of weakly magnetic bottom ash. Variation of the data for weakly magnetic bottom ash was also higher, so there is no difference observed between weakly magnetic and non-magnetic bottom ash. The strength was in the following order: non-magnetic ≈ weakly magnetic > as-received > strongly magnetic.

The specific strength, a ratio of compressive strength and oven dry weight, described as MPa per gram of sample, is shown in Fig. 9. For each gram of sample, plain mortar (0.1687 MPa/g) and mortar made of non-magnetic bottom ash (0.1736 MPa/g) showed higher values than mortars made of as-received (0.1314 MPa/g), strongly magnetic (0.1115 MPa/g), and weakly magnetic (0.1372 MPa/g) bottom ash. Although the mechanical strength of mortar with non-magnetic bottom ash was smaller than that of plain mortar (Fig. 8), mortar made of non-magnetic bottom ash showed higher specific strength that that of plain mortar (Fig. 9). This result indicates that non-magnetic

Table 7 Evaluation of pozzolanic activity by conductivity measurement (Luxán et al., 1989)

Classification of material	Variation on conductivity according to proposed method (mS/cm)
Non pozzolanic	Less than 0.4
Variable pozzolanicity	Between 0.4 and 1.2
Good pozzolanicity	Greater than 1.2

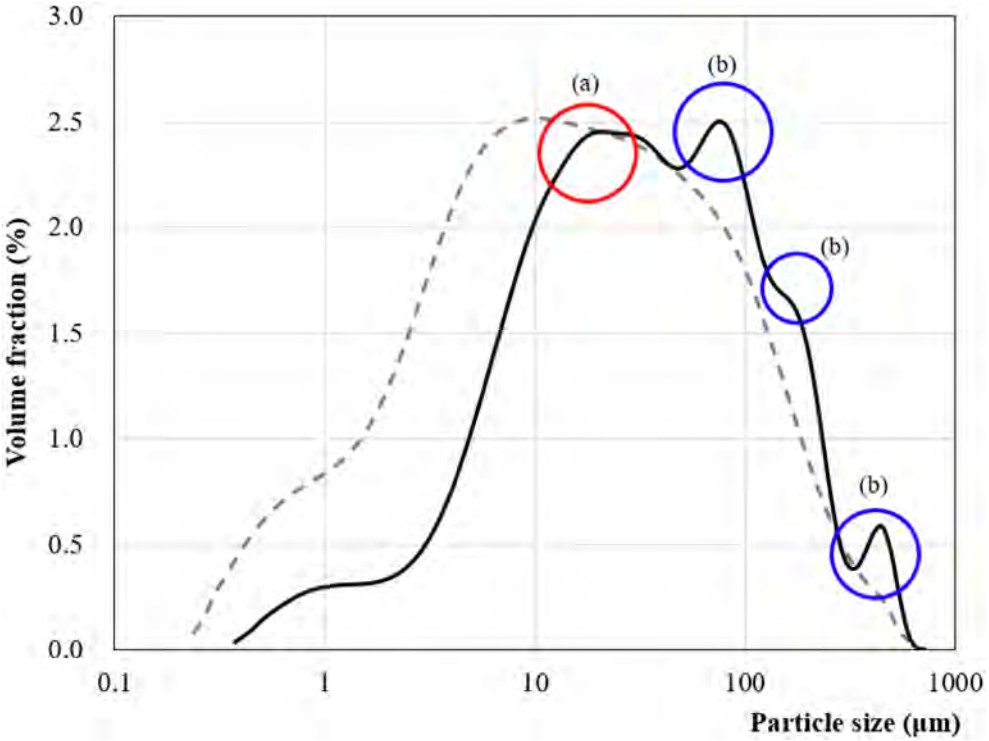

Fig. 7 The particle size distribution curve of fly ash obtained from Hadong pond site. Note that black solid line indicates fly ash obtained from Hadong pond site and black the dotted line indicates typical class F fly ash with similar chemical and mineralogical compositions: (**a**) shape similar to fly ash and (**b**) particle agglomeration

bottom ash can perform similar level of load bearing capability in terms of unit weight, suggesting that it can be successfully used as a source of lightweight aggregate.

3.2.2 Water Absorption

Water absorption of mortar made of magnetically separated bottom ashes are presented in Table 8. The water absorption capacity determined from the increase in weight of surface dry samples after being submerged for 24 h. As expected, mortar made of standard sand showed the lowest absorption. Water absorption of mortars made of bottom ash was in the order of non-magnetic (11.08%) > as-received (10.53%) > weakly magnetic (9.97%) > strongly magnetic (9.32%), which were approximately 2 times as high as that of mortar made of standard sand. Although there is slight discrepancy between as-received and weakly magnetic bottom ash, water absorption of mortar made of magnetically separated bottom ash generally followed the trend of absorption capacity of bottom ash that are presented in Table 8. However, there is no clear correlation between total water absorption of mortar and total porosity of bottom ash.

3.2.3 Thermal Conductivity

Thermal conductivity of mortar specimen (100 × 50 × 20 mm) measured at 28 days is presented in Fig. 10. Thermal conductivity of plain mortar was 2.71 W/m·K. Thermal conductivity of mortar made of as-received bottom ash was 0.96 W/m·K. Approximately 65% reduction in thermal conductivity, which is associated with highly porous microstructure of bottom ash, can be obtained. Thermal conductivities of mortars made of strongly magnetic and weakly magnetic bottom ashes were 1.10 and 1.02 W/m K, respectively, and they were higher than that made of as-received and non-magnetic bottom ash. Mortar made of non-magnetic bottom ash showed the lowest thermal conductivity of 0.89 W/m K. It is because mortars made of strongly magnetic and weakly magnetic bottom ash contains higher amount of magnetite and hematite, and thus provided higher thermal conductivity within its microstructure although they had higher porosity than non-magnetic bottom ash.

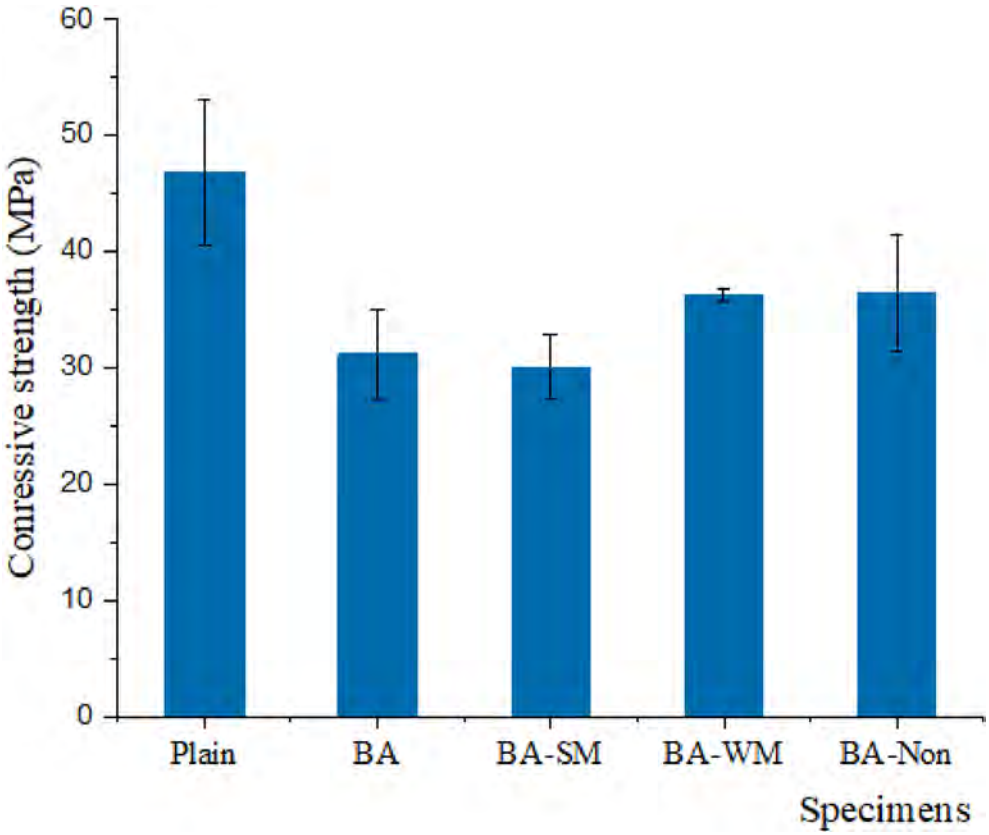

Fig. 8 The 28 day compressive strengths of mortar specimen made of bottom ash

4 Industrial Scale Experiments and Results (A Case Study)

In this section, experimental procedure used for the production of masonry cement brick using magnetically separated bottom ash is described. The properties of masonry cement brick made of magnetically separated bottom ash are investigated as well.

4.1 Industrial Scale Experimental Procedure

The production of masonry cement brick was performed in a production factory of Daewangcon Co. Ltd., located at Chirwon, Republic of Korea. First, as-received bottom ash was magnetically separated using 3000 gauss magnetic rod, and magnetic (both strongly and weakly magnetic) bottom ash samples were used as lightweight aggregate. Although the performance of magnetic bottom ash from lab-scale experiment was lower than that of non-magnetic bottom ash in terms of strength development and thermal conductivity, magnetic bottom ash was used because of its lower unburnt carbon content. It should be noted that separation of unburnt carbon content from non-magnetic bottom ash was unable to be applied because it was difficult to completely separate all unburnt carbon contents from large amount of non-magnetic bottom ash at the production factory. Therefore, masonry cement brick with non-magnetic bottom ash was not produced.

Ordinary type I portland cement was used for production of masonry cement brick using an industrial scale apparatus. The size of masonry cement brick was 190×90×57 mm. Mix proportions of cement masonry brick are presented in Table 9. Two different cement contents, 30 and 24 kg, were used to prepare cement masonry brick. Cement and bottom ash were first added to the mixer and water was added later. Water content was adjusted until fresh mortar mixture met the required consistency level that can be fed into the brick production line. After mixing, fresh mortar mixture was poured into the mold, vibration was applied for approximately 5 ~ 10 s, and molds were removed as presented in Fig. 11a. Masonry cement brick samples were moved (Fig. 11b) to the steam curing facility, and steam cured at 60 °C for 24 h. After steam curing, masonry cement bricks were taken out to the storage site until it met 7 days of total curing time. Photographic images of produced masonry cement brick, dimension, and loading for compressive strength test are presented in Fig. 11c–e.

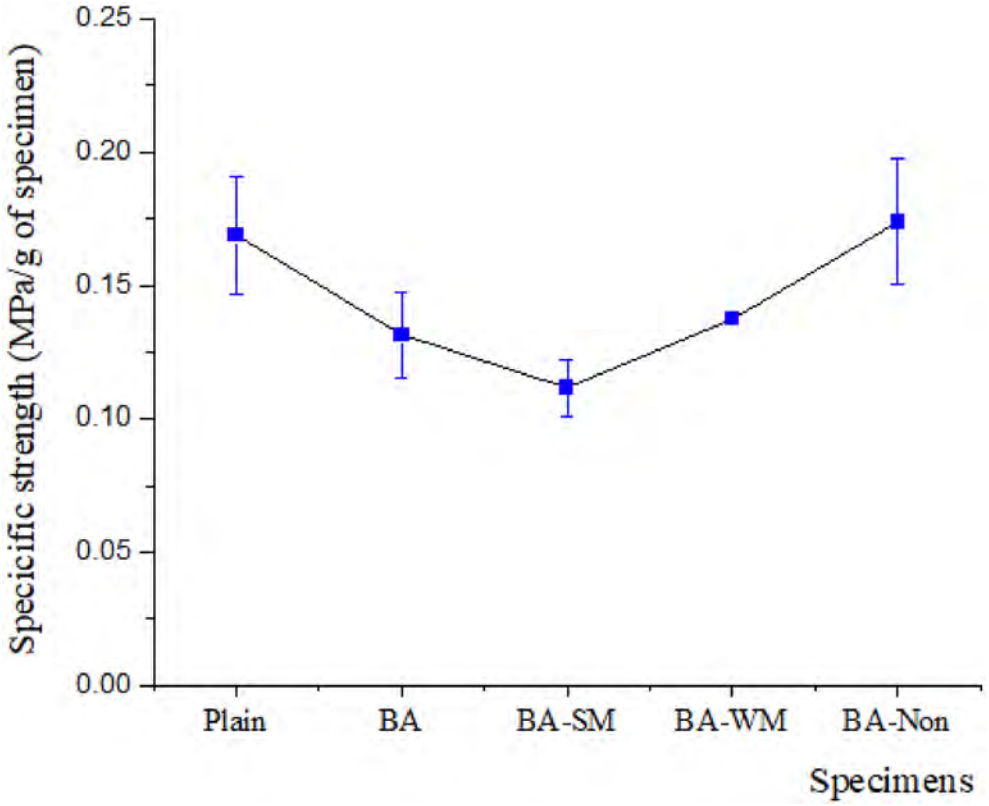

Fig. 9 Specific strengths (compressive strength divided by oven dry weight) of mortar specimen made of bottom ash

Table 8 Absorption of plain and bottom ash-substituted cement mortar

Bottom ash Properties	Plain	As-received	Strongly magnetic	Weakly magnetic	Non-magnetic
Absorption capacity (%)	4.97	10.53	9.32	9.97	11.08

At 7 days after production of masonry cement brick, compressive strength (ASTM C 67), absorption capacity (ASTM C 67), bulk specific gravity (ASTM C 128), unit weight (ASTM C 128) (ASTM C67–03, 2004), and thermal conductivity (ASTM C 1113) of masonry cement brick made of as-received and non-magnetic bottom ash were measured. LFor comparison of the results, the above-mentioned properties of masonry brick samples that was made of sand in the same factory were evaluated.

4.2 Properties of Masonry Cement Brick

Fig. 12 shows the 7 day compressive strength of masonry cement bricks made of as-received and magnetically separated bottom ash. Masonry cement brick made of as-received bottom ash showed the lowest compressive strength of 4.87 MPa. Masonry cement brick made of magnetic bottom ash showed compressive strengths of 12.53 MPa (for C30 mixture) and 8.96 MPa (for C24 mixture). Both C30 and C24 mixtures met the required strength of 8 MPa, which is the qualified strength level for second class masonry brick (KS F4004, 2013). However, the strengths were lower than masonry cement brick made of sand.

It was clear that masonry cement brick with higher cement content showed higher compressive strength. The difference in compressive strength between bricks made of as-received bottom ash and bricks made of magnetic bottom ash was approximately 2 ~ 3 times higher for bricks made of magnetic bottom ash. It was mostly associated with the presence of unburnt carbon (preventing effective binding of bottom ash) that was present in as-received bottom ash.

When specific strengths of masonry cement bricks, shown in Fig. 13, are compared, except for the case of as-received bottom ash whose unburnt carbon content were not removed, both C30 and C24 mixtures showed specific strengths of 0.01138 and 0.00836 MPa/g, which were higher or almost identical to that of masonry cement brick made of standard sand (0.00878 MPa/g).

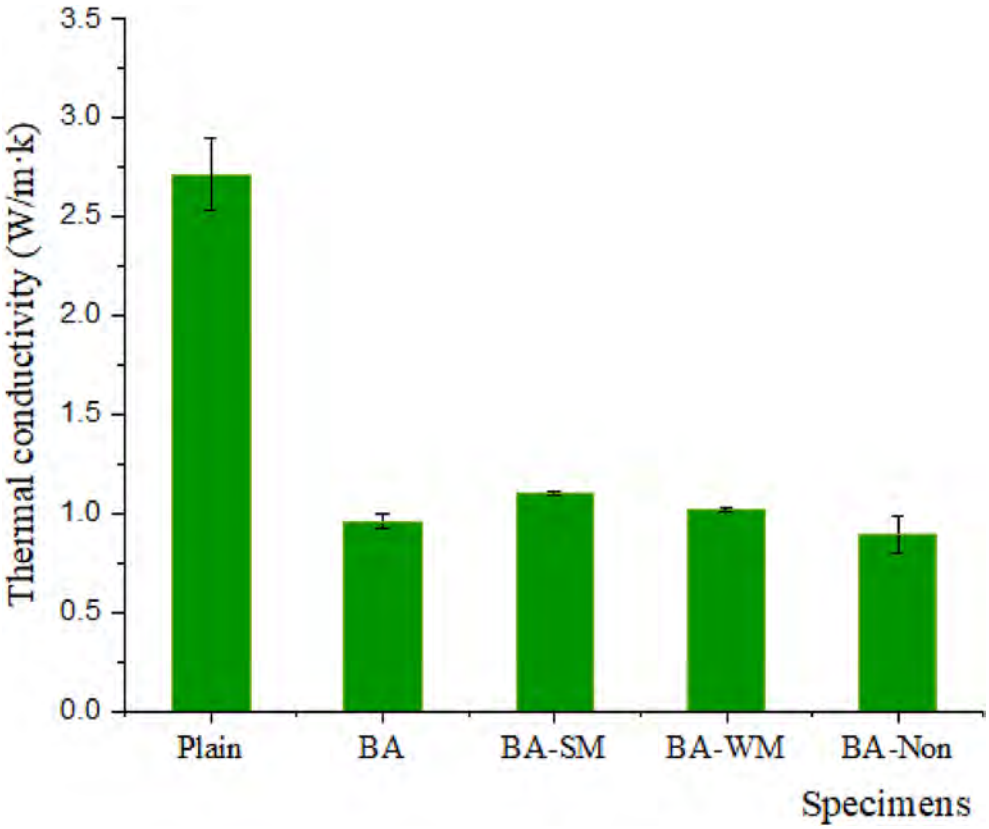

Fig. 10 Thermal conductivities of mortar made of magnetically separated bottom ash

Table 9 Mix proportions of cement masonry brick

No	Sample	Water (kg)	Cement (kg)	Bottom ash
1	C30-as-received	25.9	30.0	67.3
2	C30-magnetic	25.9	30.0	67.3
3	C24-magnetic	26.95	24.0	67.3

The result indicates that magnetically separated bottom ash can also be effectively used as a source of lightweight aggregate for masonry cement brick production.

According to Table 10, absorption capacities of masonry cement bricks made of magnetic bottom ash samples were 26.55% (for C30 mixture) and 28.67% (for C24 mixture), respectively. These values were approximately 2 ~ 3 times higher than the absorption capacity of cement bricks made of natural sand (11.27%). Bulk specific gravities of cement brick made of bottom ash samples were 30% lower than that made of natural sand. Unit weights of cement brick made of bottom ash samples were 40% lower than that made of natural sand. Thermal conductivity of the brick made of magnetic bottom ash was 20% lower than that made of natural sand. The results strongly suggest that masonry cement brick made of magnetic bottom ash can be used as a lightweight cement brick that can increase heat insulation.

5 Discussion

In this work, bottom ash that was in the range of 0.075 ~ 4.75 mm were used. Bottom ash whose size was larger than 4.75 mm was not used because heavier bottom ash cannot be effectively separated using a magnet with intermediate strength level. Bottom ash that has smaller particle size was not considered for utilization, either. It was because those bottom ash contained large amount of unburnt carbon and it could negatively affect the properties of mortar when used as a lightweight aggregate.

The effect of unburnt carbon for production of lightweight masonry cement brick was clearly presented from the results shown in Fig. 8 (from a laboratory-scale experiments) and Fig. 12 (from an industrial-scale experiment). According to Fig. 8, mortar made of as-received bottom ash whose unburnt carbon content was removed prior to the preparation of mortar did not show clear reduction in compressive strength. However, according to Fig. 12,

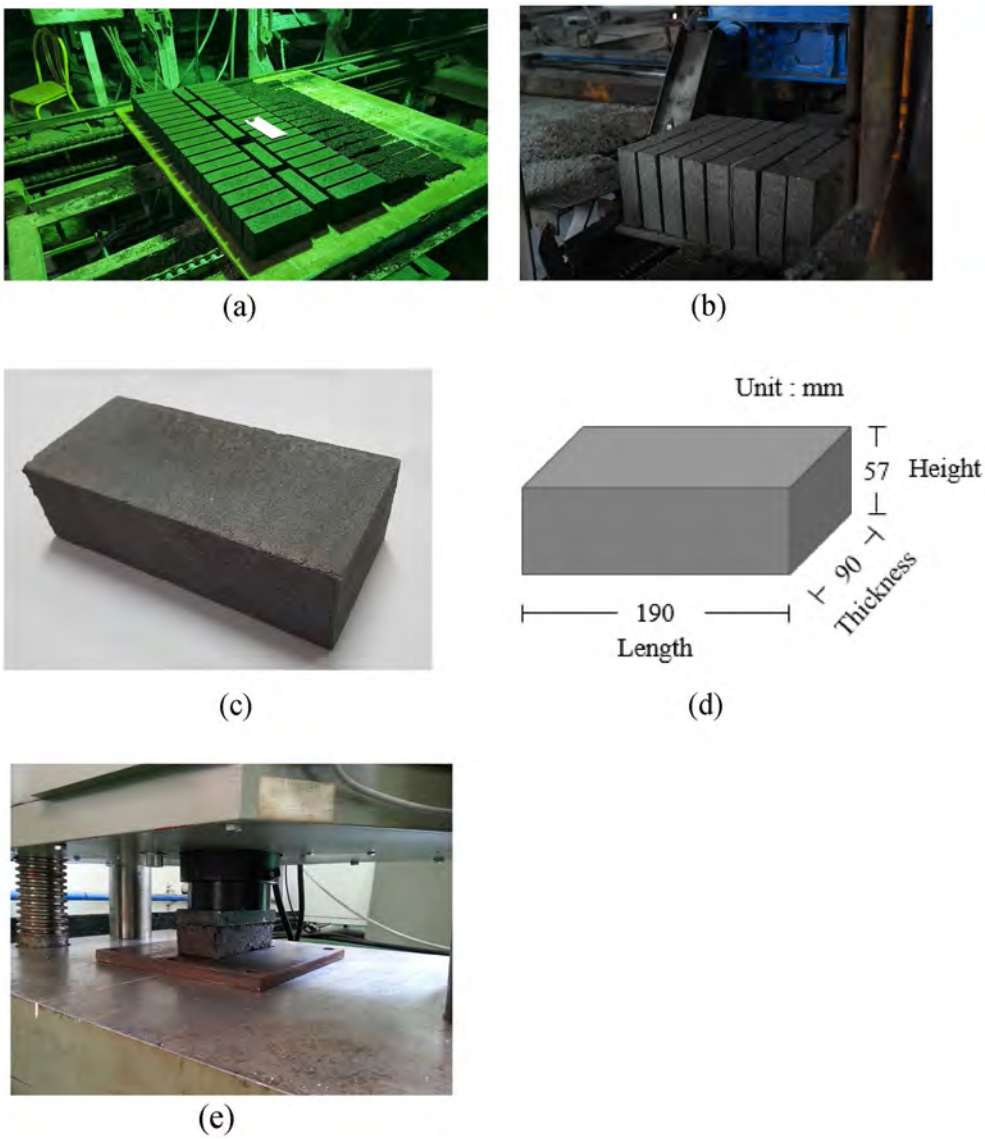

Fig. 11 Photographic images of masonry cement brick: (**a**) immediately after demolding, (**b**) moving to a curing facility, (**c**) after curing, (**d**) dimension, and (**e**) loading for compressive strength test

masonry cement brick made of as-received bottom ash (C30-as-received) whose unburnt carbon content was not removed showed a huge reduction (approximately 70%) in compressive strength compared to the strength of masonry cement brick made of magnetic bottom ash (C30-magnetic) that had the same mix proportions. The results suggest that the removal of unburnt carbon from bottom ash is a prior task. Since there are several techniques available for efficient separation of unburnt carbon content from bottom ash (Cruceru et al., 2019; Kim et al., 2022; Şahbaz et al., 2008; Valeev et al., 2019; Xing et al., 2019), the application of such techniques on bottom ash needs to be followed in order for a complete utilization of abondoned bottom ash. Removed (or separated) unburnt carbon can be successfully recycled as a raw ingredient for production of electricity in a coal fired power plant. Bottom ash can also be successfully utilized as a lightweight aggregate. If unburnt carbon content in bottom ash cannot be removed due to the various on-site issues, bottom ash should be at least magnetically separated to be used as aggregate for production of cementitious composites.

Since non-magnetic bottom ash consists of the majority of as-received bottom ash, successful utilization of non-magnetic bottom ash would be a key issue for complete recycling of bottom ash. From the results obtained

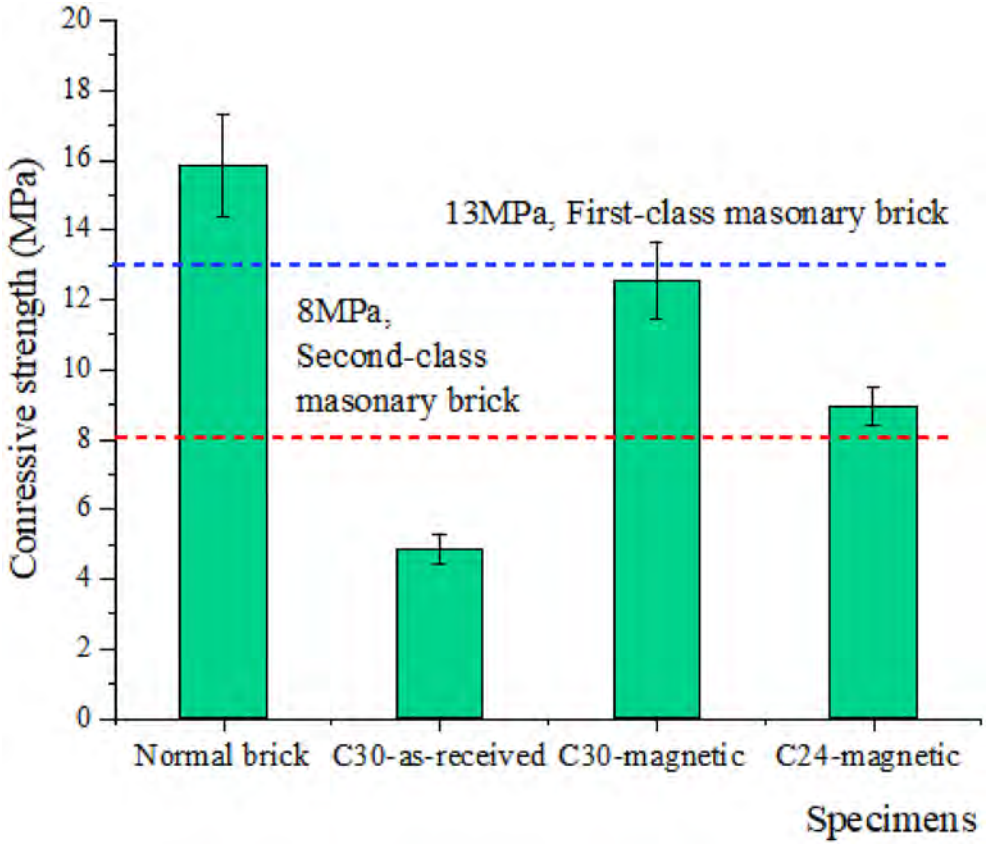

Fig. 12 The 7 day compressive strength of masonry cement bricks made of as-received and magnetically separated bottom ash

from the laboratory-scale experiments, mortar made of non-magnetic bottom ash showed higher compressive strength and specific strength (Figs. 8 and 9) with reduced thermal conductivity (Fig. 10) than magnetic bottom ash. From the results obtained from the industrial-scale experiments, masonry cement bricks made of magnetic bottom ash showed higher or identical specific strengths (Fig. 13) with reduced thermal conductivity (Table 10) than that made of standard sand (Fig. 13). If unburnt carbon content from non-magnetic bottom ash were removed and used for industrial-scale experiments, masonry cement brick made of non-magnetic bottom ash would have been produced and the properties of brick would have been better than those made of magnetic bottom ash. Removal of unburnt carbon and utilization of non-magnetic bottom ash are the ideal case for complete recycling of abandoned bottom ash.

According to the Fig. 8, strongly magnetic bottom ash was found to be not as much applicable as non-magnetic bottom ash in terms of production of lightweight cementitious material due to its relatively lower strength with higher thermal conductivity compared to non-magnetic bottom ash. However, considering the amount of Fe_2O_3 content in strongly magnetic and weakly magnetic bottom ashes (35 ~ 40%), they can be successfully utilized as a source material for other industries (Han et al., 2009; Valeev et al., 2019). Such application may introduce higher value than just utilizing magnetic bottom ash as source of lightweight aggregate. Further research needs to be performed to maximize the applicability of magnetic bottom ash.

According to the experimental results obtained in this work, the magnetic separation process using 1000 and 3000 gauss magnets was found to be effective for bottom ash whose particle size was in the range of 0.075 ~ 5 mm. However, the use of two different magnets for separation of strongly magnetic and weakly magnetic bottom ash was not found to be an essential process as it was originally expected. The amount of weakly magnetic bottom ash was only 1.88% for particle sizes around 0.853 ~ 5 mm and 3.79% for particle sizes around 0.075 ~ 0.853 mm, respectively. The amount is so small that the effect of weakly magnetic bottom ash cannot cause significant impact on the properties of mortar or brick made of magnetic bottom ash. Removal of either 1000 gauss or 3000 gauss magnet

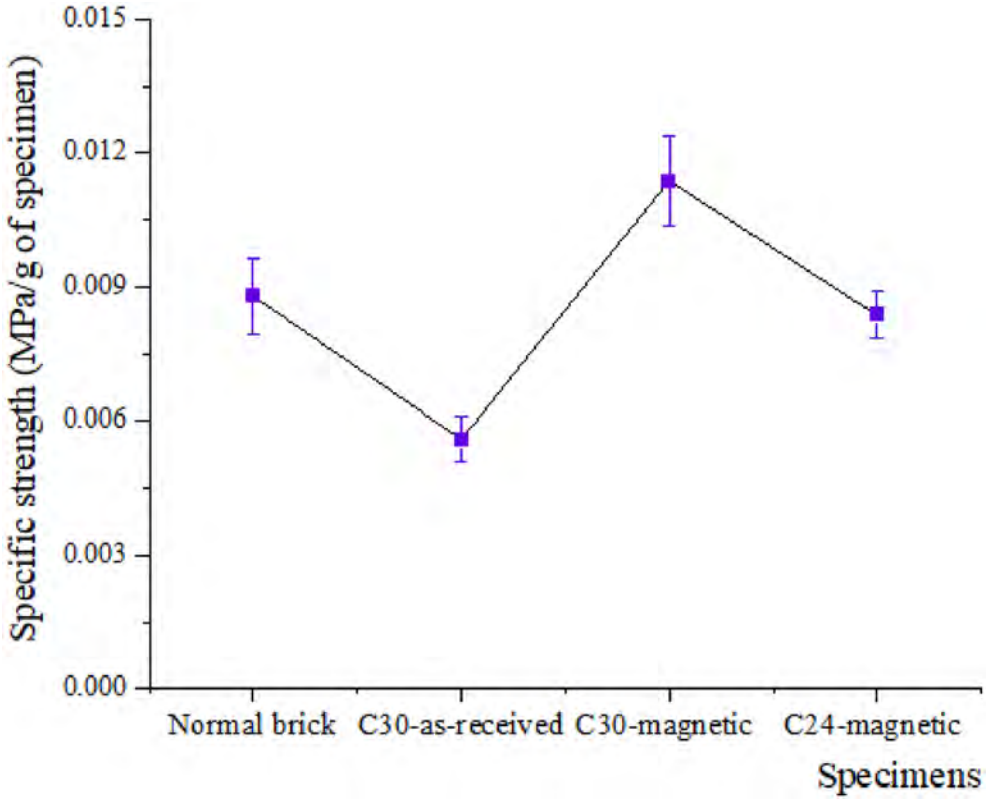

Fig. 13 Specific strengths (compressive strength divided by oven dry weight) of masonry cement bricks of made of as-received and magnetically separated bottom ash

Table 10 Properties of masonry cement brick made of bottom ash

No	Sample	Oven dry bulk specific gravity (g/cm^3)	Absorption capacity (%)	Oven dry unit weight (g/cm^3)	Thermal conductivity (in air dry condition) (W/m·K)
1	Normal brick (natural sand)	2.51	11.27	1.85	0.64
2	C30-as-received	1.75	30.20	1.12	0.55
3	C30-magnetic	1.77	26.55	1.13	0.53
4	C24-magnetic	1.78	28.67	1.10	0.52

is highly recommended for easier and more economic separation process.

6 Conclusion

In this work, magnetic separation was applied on bottom ash that was stored in the pond site of Hadong coal fired power plant. Properties of magnetically separated bottom ash were analyzed, mortar specimens as well as masonry cement brick samples were prepared, and compressive strength, water absorption, and thermal conductivity were measured. According to the results obtained from this work, following conclusions can be drawn.

1) Magnetic separation with 1000 and 3000 gauss magnet was effective for separating bottom ash samples that contains higher amount of magnetite. As a result, bulk and skeletal density of strongly magnetic bottom ash were higher than those of as-received bottom ash. Non-magnetic bottom ash showed the lowest bulk and skeletal density.
2) Pozzolanic activity of bottom ash was ranged 53 ~ 62% of fly ash that was stored at the same pond site. Considering the particle agglomeration observed from the fly ash, it is possible to evaluate the pozzolanic activity of bottom ash either as non-pozzolanic or as very weakly pozzolanic.

3) From laboratory scale experiments, non-magnetic bottom ash showed the better performance than strongly magnetic bottom ash in terms of compressive strength and thermal conductivity. Since large amount of unburnt carbon stayed together with non-magnetic bottom ash, removal of unburnt carbon is a key factor for successful utilization of non-magnetic bottom ash.
4) Masonry cement brick made of magnetic bottom ash showed 40% reduction in unit weight, 20% reduction in thermal conductivity. Utilization of non-magnetic bottom ash for masonry cement brick production after removal of unburnt carbon can also be a successful application, considering the results from laboratory-scale experiments (density and thermal conductivity was lower for non-magnetic bottom ash).

Acknowledgements
This work is supported by the Korea Agency for Infrastructure Technology Advancement (KAIA) grant funded by the Ministry of Land, Infrastructure and Transport (Grant 23NANO-C156177-04).

Author contributions
Prof. JHK: Writing—Original Draft, Writing—Review & Editing, Formal analysis, conceptualization, Investigation. Dr. HM: Investigation, Methodology, Writing—Review & Editing, Formal analysis. Prof. CWC: Funding acquisition, Project administration, Conceptualization, Methodology, Formal analysis, Writing—Review & Editing.

Funding
Korea Agency for Infrastructure Technology Advancement (KAIA) grant funded by the Ministry of Land, Infrastructure and Transport (Grant 23NANO-C156177-04). Authors appreciate all the members in Daewangcon Co. Ltd. for their kind support provided during this project.

Availability of data and materials
The datasets used and/or analyzed during the current study are available from the corresponding author on reasonable request.

Declarations

Competing interests
The authors declare that they have no competing interests.

Received: 4 October 2023 Accepted: 9 December 2023
Published online: 08 April 2024

References

Abbas, S., Arshad, U., Abbass, W., Nehdi, M. L., & Ahmed, A. (2020). Recycling untreated coal bottom ash with added value for mitigating alkali–silica reaction in concrete: a sustainable approach. *Sustainability, 12*(24), 10631. https://doi.org/10.3390/su122410631

Alyaseen, A., Poddar, A., Alahmad, H., Kumar, N., & Sihag, P. (2023). High-performance self-compacting concrete with recycled coarse aggregate: comprehensive systematic review on mix design parameters. *Journal of Structural Integrity and Maintenance, 8*(3), 161–178. https://doi.org/10.1080/24705314.2023.2211850

Andrade, L. B. (2004). *Methodology of assessment to use of bottom ash of thermoelectric power plants as aggregate in concrete*. Brazil: Department of Civil Engineer, Federal University of Santa Catarina.

Andrade, L. B., Rocha, J. C., & Cheriaf, M. (2007). Evaluation of concrete incorporating bottom ash as a natural aggregates replacement. *Waste Management, 27*, 1190–1199. https://doi.org/10.1016/j.wasman.2006.07.020

ASTM C1113–90. (2013). *Test method for thermal conductivity of refractories by hot wire (platinum resistance thermometer technique), American society for testing and materials*. West Conshohocken: ASTM International.

ASTM C305, 2006, Standard Practice for Mechanical Mixing of Hydraulic Cement Pastes and Mortars of Plastic Consistency, Annual Book of ASTM Standards, Vol. 04.01, ASTM International. West Conshohocken.

ASTM C109. (2008). *Standard test method for compressive strength of hydraulic cement mortars*. West Conshohocken: ASTM International.

ASTM C128. (2015). *Standard test method for density for relative density (specific gravity) and absorption*. West Conshohocken: ASTM international.

ASTM C150. (2009). *Standard specification for Portland cement*. West Conshohocken: ASTM international.

ASTM C67–03. (2004). *Standard test methods for sampling and testing brick and structural clay tile, American society for testing and materials*. West Conshohocken: ASTM International.

Atiş, C. D. (2002a). Heat evolution of high-volume fly ash concrete. *Cement and Concrete Research, 32*(5), 751–756. https://doi.org/10.1016/S0008-8846(01)00755-4

Atiş, C. D. (2002b). Heat evolution of high-volume fly ash concrete. *Cement and Concrete Research, 32*, 751–756. https://doi.org/10.1016/S0008-8846(01)00755-4

Bui, N. K., Satomi, T., & Takahashi, H. (2019). Influence of industrial by-products and waste paper sludge ash on properties of recycled aggregate concrete. *Journal of Cleaner Production, 214*, 403–418. https://doi.org/10.1016/j.jclepro.2018.12.325

Caprai, V., Schollbach, K., Florea, M. V. A., & Brouwers, H. J. H. (2020). Investigation of the hydrothermal treatment for maximizing the MSWI bottom ash content in fine lightweight aggregates. *Construction and Building Materials, 230*, 116947. https://doi.org/10.1016/j.conbuildmat.2019.116947

Cheriaf, M., Cavalcante Rocha, J., & Péra, J. (1999). Pozzolanic properties of pulverized coal combustion bottom ash. *Cement and Concrete Research, 29*, 1387–1391. https://doi.org/10.1016/S0008-8846(99)00098-8

Chimenos, J. M., Segarra, M., Ferna´ndez, M. A., & Espiell, F. (1999). Characterization of the bottom ash in municipal solid waste incinerator. *Journal of Hazardous Materials A, 64*, 211–222. https://doi.org/10.1016/S0304-3894(98)00246-5

Chimenos, J. M., Segarra, M., Fernández, M., & Espiell, F. (1999a). Characterization of the bottom ash in municipal solid waste incinerator. *Journal of Hazardous Materials, 64*(3), 211–222. https://doi.org/10.1016/S0304-3894(98)00246-5

Chindaprasirt, P., Jaturapitakkul, C., Chalee, W., & Rattanasak, U. (2009). Comparative study on the characteristics of fly ash and bottom asf geopolymers. *Waste Management, 29*, 539–543. https://doi.org/10.1016/j.wasman.2008.06.023

Choi, I. J., Kim, J. H., & Lee, S. Y. (2016). Evaluation on reactivity of by-product pozzolanic materials using electrical conductivity measurement. *Journal of the Korea Institute of Building Construction, 16*(5), 421–428. https://doi.org/10.5345/JKIBC.2016.16.5.421

Çiçek, T., & Çinçin, Y. (2015). Use of fly ash in production of light-weight building bricks. *Construction and Building Materials, 94*, 521–527. https://doi.org/10.1016/j.conbuildmat.2015.07.029

Cruceru, M., Diaconu, B. M., Valentim, B., & Anghelescu, L. (2019). A process flow for extraction of unburned carbon from bottom ash-economical and environmental assessment. *International Multidisciplinary Scientific GeoConference: SGEM, 19*(4.1), 645–652. https://doi.org/10.5593/sgem2019/4.1

De Boom, A., Degrez, M., Hubaux, P., & Lucion, C. (2011). MSWI boiler fly ashes: magnetic separation for material recovery. *Waste Management, 31*(7), 1505–1513. https://doi.org/10.1016/j.wasman.2011.01.002

de Matos, P. R., Junckes, R., Graeff, E., & Prudencio, L. R., Jr. (2020). Effectiveness of fly ash in reducing the hydration heat release of mass concrete. *Journal of Building Engineering, 28*, 101063. https://doi.org/10.1016/j.jobe.2019.101063

Filipponi, P., Polettini, A., Pomi, R., & Sirini, P. (2003). Physical and mechanical properties of cement-based products containing incineration bottom ash. *Waste Management, 23*(2), 145–156. https://doi.org/10.1016/S0956-053X(02)00041-7

Ghafoori, N., & Bucholc, J. (1996). Investigation of lignite-based bottom ash for structural concrete. *Journals of Materials in Civil Engineering, 8*, 128–137. https://doi.org/10.1061/(ASCE)0899-1561(1996)8:3(128)

Han, G. C., Um, N. I., You, K. S., Cho, H. C., & Ahn, J. W. (2009). Recovery of ferromagnetic material by wet magnetic separation in coal bottom ash. *Geosystem Engineering, 12*(1), 9–12. https://doi.org/10.1080/12269328.2009.10541292

Han, M. C., Han, D., & Shin, J. K. (2015). Use of bottom ash and stone dust to make lightweight aggregate. *Construction and Building Materials, 99*, 192–199. https://doi.org/10.1016/j.conbuildmat.2015.09.036

Hussain, S., Bhunia, D., Singh, S. B., & Yadav, J. S. (2022). A study on the carbonation of binary and ternary blended cement mortar and concrete. *Journal of Structural Integrity and Maintenance, 7*(1), 46–60. https://doi.org/10.1080/24705314.2021.1971892

International Energy Agency. (2009). *World energy outlook* (p. 17). OECD/IEA.

Jaturapitakkul, C., & Cheerarot, R. (2003). Development of bottom ash as pozzolanic material. *Journal of Materials in Civil Engineering, 15*, 48–53. https://doi.org/10.1061/(ASCE)0899-1561(2003)15:1(48)

Jurič, B., Hanžič, L., Ilić, R., & Samec, N. (2006). Utilization of municipal solid waste bottom ash and recycled aggregate in concrete. *Waste Management, 26*, 1436–1442. https://doi.org/10.1016/j.wasman.2005.10.016

Kim, M., Park, J., Kang, H., & Jeong, D. (2022). Efficiency evaluation of the bottom ash flotation collector by removed saturated fatty acids from soybean oil. *Physicochemical Problems of Mineral Processing, 58*(1), 126–137. https://doi.org/10.3719/ppmp/144775

Korre, A., Nie, Z., & Durucan, S. (2010). Life cycle modelling of fossil fuel power generation with post-combustion CO_2 capture. *International Journal of Greenhouse Gas Control, 4*(2), 289–300. https://doi.org/10.1016/j.ijggc.2009.08.005

KS L ISO 679. 2006. Methods of Testing Cements-Determination of Strength. Korean Standards Service Network, Korean Standards Association (ISO code 91.100.10).

KS F 2459, 2002, Testing Methods for Density, Water Content, Absorption and Compressive Strength of Celluar Concrete, Korean Standards Service Network, Korean Standards Association (ISO code 91.100.30).

KS F 4004, 2013, Concrete Brick, Korean Standards Service Network, Korean Standards Association

Kula, I., Olgun, A., Sevinc, V., & Erdogan, Y. (2002). An investigation on the use of tincal ore waste, fly ash, and coal bottom ash as Portland cement replacement materials. *Cement and Concrete Research, 32*, 227–232. https://doi.org/10.1016/S0008-8846(01)00661-5

Kumar, S., & Rai, B. (2022). Synergetic effect of fly ash and silica fume on the performance of highvolume fly ash self-compacting concrete. *Journal of Structural Integrity and Maintenance, 7*(1), 61–74. https://doi.org/10.1080/24705314.2021.1892571

Langan, B. W., Weng, K., & Ward, M. A. (2002). Effect of silica fume and fly ash on heat of hydration of portland cement. *Cement and Concrete Research, 32*(7), 1045–1051. https://doi.org/10.1016/S0008-8846(02)00742-1

Leblond, D. (2006). Iea: fossil energy to dominate market through 2030. *Oil & Gas Journal, 104*(43), 28–29.

Lee, H., Hanif, A., Usman, M., Kim, Y., Oh, H., & Kim, S. K. (2020). Interfacial characteristics of cement mortars containing aggregate derived from industrial slag waste. *Journal of Structural Integrity and Maintenance, 5*(4), 236–243. https://doi.org/10.1080/24705314.2020.1783124

Leung, H. Y., Kim, J., Nadeem, A., Jaganathan, J., & Anwar, M. P. (2016). Sorptivity of self-compacting concrete containing fly ash and silica fume. *Construction and Building Materials, 113*, 369–375. https://doi.org/10.1016/j.conbuildmat.2016.03.071

Liu, Y., Sidhu, K. S., Chen, Z., & Yang, E. H. (2018). Alkali-treated incineration bottom ash as supplementary cementitious materials. *Construction and Building Materials, 179*, 371–378. https://doi.org/10.1016/j.conbuildmat.2018.05.231

Luxán, M. P., Madruga, F., & Saavedra, J. (1989). Rapid evaluation of pozzolanic activity of natural products by conductivity measurement. *Cement and Concrete Research, 19*(1), 63–68. https://doi.org/10.1016/0008-8846(89)90066-5

Mangi, S. A., Ibrahim, M. H. W., Jamaluddin, N., Arshad, M. F., Memon, F. A., Jaya, R. P., & Shahidan, S. (2018). A review on potential use of coal bottom ash as a supplementary cementing material in sustainable concrete construction. *International Journal of Integrated Engineering, 10*(9), 28–36. https://doi.org/10.3088/ijie.2018.10.09.006

Meek, H., Elchalakani, M., Beckett, C. T., & Dong, M. (2021). Alternative stabilised rammed earth materials incorporating recycled waste and industrial by-products: a study of mechanical properties, flexure and bond strength. *Construction and Building Materials, 277*, 122303. https://doi.org/10.1016/j.conbuildmat.2021.122303

MØlgaard, J., & Smeltzer, W. W. (1971). Thermal conductivity of magnetite and hematite. *Journal of Applied Physics, 42*(9), 3644–3647. https://doi.org/10.1063/1.1660785

Moon, H., Kim, J. H., Lee, J. Y., Kim, S. G., & Chung, C. W. (2017). Evaluation of pozzolanic activity for effective utilization of dredged sea soil. *International Journal of Concrete Structures and Materials, 11*(4), 637–646. https://doi.org/10.1007/s40069-017-0215-6

Moradllo, M. K., Chung, C. W., Keys, M. H., Choudhary, A., Reese, S. R., & Weiss, W. J. (2020). Use of borosilicate glass powder in cementitious materials: Pozzolanic reactivity and neutron shielding properties. *Cement and Concrete Composites, 112*, 103640.

Nocuń-Wczelik, W. (2001). Heat evolution in hydrated cementitious systems admixtured with fly ash. *Journal of Thermal Analysis and Calorimetry, 65*, 613–619. https://doi.org/10.1023/A:1017970228316

Nyale, S. M., Babajide, O. O., Birch, G. D., Böke, N., & Petrik, L. F. (2013). Synthesis and characterization of coal fly ash-based foamed geopolymer. *Procedia Environmental Sciences, 18*, 722–730. https://doi.org/10.1016/j.proenv.2013.04.098

Oakes, L., Magee, B., McIlhagger, A., & McCartney, M. (2019). Strength prediction and mix design procedures for geopolymer and alkali-activated cement mortars comprising a wide range of environmentally responsible binder systems. *Journal of Structural Integrity and Maintenance, 4*(3), 135–143. https://doi.org/10.1080/24705314.2019.1622189

Pala, M., Özbay, E., Öztaş, A., & Yuce, M. I. (2007). Appraisal of long-term effects of fly ash and silica fume on compressive strength of concrete by neural networks. *Construction and Building Materials, 21*, 384–394. https://doi.org/10.1016/j.conbuildmat.2005.08.009

Paya, J., Borrachero, M. V., Monzó, J., Peris-Mora, E., & Amahjour, F. (2001). Enhanced conductivity measurement techniques for evaluation of fly ash pozzolanic activity. *Cement and Concrete Research, 31*(1), 41–49.

Rafieizonooz, M., Mirza, J., Salim, M. R., Hussin, M. W., & Khankhaje, E. (2016). Investigation of coal bottom ash and fly ash in concrete as replacement for sand and cement. *Construction and Building Materials, 116*, 15–24. https://doi.org/10.1016/j.conbuildmat.2016.04.080

Şahbaz, O., Öteyaka, B., Kelebek, Ş, Uçar, A., & Demir, U. (2008). Separation of unburned carbonaceous matter in bottom ash using Jameson cell. *Separation and Purification Technology, 62*(1), 103–109. https://doi.org/10.1016/j.seppur.2008.01.005

Sathonsaowaphak, A., Chindaprasirt, P., & Pimraksa, K. (2009). Workability and strength of lignite bottom ash geopolymer mortar. *Journal of Hazardous Materials, 168*(1), 44–50. https://doi.org/10.1016/j.jhazmat.2009.01.120

Schindler, A. K., & Folliard, K. J. (2005). Heat of hydration models for cementitious materials. *ACI Materials Journal, 102*(1), 24.

Shafiee, S., & Topal, E. (2008). An econometrics view of worldwide fossil fuel consumption and the role of US. *Energy Policy, 36*(2), 775–786. https://doi.org/10.1016/j.enpol.2007.11.002

Siddique, R. (2003). Effect of fine aggregate replacement with class F fly ash on the mechanical properties of concrete. *Cement and Concrete Research, 33*, 539–547. https://doi.org/10.1016/S0008-8846(02)01000-1

Šulc, R., Šídlová, M., Formáček, P., Snop, R., Škvára, F., & Polonská, A. (2022). A study of physicochemical properties of stockpile and ponded coal ash. *Materials, 15*(10), 3653. https://doi.org/10.3390/ma15103653

Suraneni, P., & Weiss, J. (2017). Examining the pozzolanicity of supplementary cementitious materials using isothermal calorimetry and thermogravimetric analysis. *Cement and Concrete Composites, 83*, 273–278.

Tikalsky, P. J., Carrasquillo, P. M., & Carrasquillo, R. L. (1988). Strength and durability considerations affecting mix proportioning of concrete containing fly ash. *ACI Materials Journal, 85*, 505–511. https://doi.org/10.1435/2260

Tran, N., Saengsoy, W., & Tangtermsirikul, S. (2021). Self-healing behavior of expansive mortars with fly ash and bottom ash. *Engineering Journal, 25*(2), 121–133. https://doi.org/10.4186/ej.2021.25.2.121

Um, N. I., Han, G. C., You, K. S., & Ahn, J. W. (2009). Immobilization of Pb, Cd and Cr by synthetic NaP1 zeolites from coal bottom ash treated by density separation. *Resources Processing, 56*(3), 130–137. https://doi.org/10.4144/rpsj.56.130

Uysal, M., Yilmaz, K., & Ipek, M. (2012). The effect of mineral admixtures on mechanical properties, chloride ion permeability and impermeability of self-compacting concrete. *Construction and Building Materials, 27*(1), 263–270. https://doi.org/10.1016/j.conbuildmat.2011.07.049

Valeev, D., Kunilova, I., Alpatov, A., Mikhailova, A., Goldberg, M., & Kondratiev, A. (2019). Complex utilisation of ekibastuz brown coal fly ash: iron & carbon separation and aluminum extraction. *Journal of Cleaner Production, 218*, 192–201. https://doi.org/10.1016/j.jclepro.2019.01.342

Wei, Y., Mei, X., Shi, D., Liu, G., Li, L., & Shimaoka, T. (2017). Separation and characterization of magnetic fractions from waste-to-energy bottom ash with an emphasis on the leachability of heavy metals. *Environmental Science and Pollution Research, 24*, 14970–14979. https://doi.org/10.1007/s11356-017-9145-8

Wongkeo, W., & Chaipanich, A. (2010). Compressive strength, microstructure and thermal analysis of autoclaved and air cured structural lightweight concrete made with coal bottom ash and silica fume. *Materials Science and Engineering: A, 527*(16–17), 3676–3684. https://doi.org/10.1016/j.msea.2010.01.089

Xing, Y., Guo, F., Xu, M., Gui, X., Li, H., Li, G., Xia, Y., & Han, H. (2019). Separation of unburned carbon from coal fly ash: a review. *Powder Technology, 353*, 372–384. https://doi.org/10.1016/j.powtec.2019.05.037

Yang, K. H. (2021). Shear friction response of lightweight concrete using bottom ash aggregates and air foams. *Journal of Structural Integrity and Maintenance, 6*(1), 37–46. https://doi.org/10.1080/24705314.2020.1823557

Yao, Z. T., Ji, X. S., Sarker, P. K., Tang, J. H., Ge, L. Q., Xia, M. S., & Xi, Y. Q. (2015). A comprehensive review on the applications of coal fly ash. *Earth-Science Reviews, 141*, 105–121. https://doi.org/10.1016/j.earscirev.2014.11.016

Yin, K., Chan, W. P., Kumaran, S., Tamilselvam, O., Chen, W. Q., Latiff, N. B. M., Heberlein, S., & Lisak, G. (2021). Redistribution of mineral phases of incineration bottom ash by size and magnetic separation and its effects on the leaching behaviors. *Environmental Pollution, 290*, 118015. https://doi.org/10.1016/j.envpol.2021.118015

Zhang, B., & Poon, C. S. (2015). Use of furnace bottom ash for producing lightweight aggregate concrete with thermal insulation properties. *Journal of Cleaner Production, 99*, 94–100. https://doi.org/10.1016/j.jclepro.2015.03.007

Publisher's Note

Ji-Hyun Kim obtained her Ph.D in Architectural Engineering at Pukyong National University. After completion ofher Ph.D, she started to collaborate with Prof. Chul-Woo Chung for developent of various construction materials.Her research interests are utilization of carbon nanomaterials, decomissioning of concrete in nuclear power plant, and recycling of industrial by-products.

Hoon Moon obtained his Ph.D in Architectural Engineering at Pukyong National University under supervision ofProf. Chul-Woo Chung. After completion of his Ph.D, he joined at Korea Institute of Civil Engineering and Building Technology (KICT) as a post-doctoral researcher. He is curreltly working on CO2 capture and utilization in construction materials. His research interests are development of sustainable materials including recycling of by-products from various sources.

Chul-Woo Chung obtained his Ph.D. in Civil Engineering at University of Illinois at Urbana Champaign. He joined Pukyong National University (PKNU), Republic of Korea, in September 2012 with various research experiences on architectural as well as civil engineering materials. Before joining PKNU, Prof. Chung used to work at Pacific Northwest National Laboratory, USA, where he gained various experiences on scientific aspects of various cementitious materials. His major research area has been on the utilization of nano-materials, capture and sequestration of CO2, and recycling of industrial by-products.